

Transmission and Color-guided Network for Underwater Image Enhancement

Pan Mu

College of Computer Science & Technology
Zhejiang University of Technology
Hangzhou, China
panmu@zjut.edu.cn

Jing Fang

College of Computer Science & Technology
Zhejiang University of Technology
Hangzhou, China
211122120024@zjut.edu.cn

Haotian Qian

College of Computer Science & Technology
Zhejiang University of Technology
Hangzhou, China
201906062215@zjut.edu.cn

Cong Bai*

College of Computer Science & Technology
Zhejiang University of Technology
Hangzhou, China
congbai@zjut.edu.cn

Abstract—In recent years, with the continuous development of the marine industry, underwater image enhancement has attracted plenty of attention. Unfortunately, the propagation of light in water will be absorbed by water bodies and scattered by suspended particles, resulting in color deviation and low contrast. To solve these two problems, we propose an Adaptive Transmission and Dynamic Color guided network (named ATDCnet) for underwater image enhancement. In particular, to exploit the knowledge of physics, we design an Adaptive Transmission-directed Module (ATM) to better guide the network. To deal with the color deviation problem, we design a Dynamic Color-guided Module (DCM) to post-process the enhanced image color. Further, we design an Encoder-Decoder-based Compensation (EDC) structure with attention and a multi-stage feature fusion mechanism to perform color restoration and contrast enhancement simultaneously. Extensive experiments demonstrate the state-of-the-art performance of the ATDCnet on multiple benchmark datasets.

Index Terms—Underwater Image Enhancement, deep learning, color restoration, and contrast enhancement

I. INTRODUCTION

Underwater images play an important role in the marine industry, such as underwater archaeology [1] and underwater target detection [2]. However, due to the complexity of the underwater environment and the optical characteristics of the water body (e.g., wavelength, distance-dependent attenuation and scattering), the underwater image will inevitably suffer from degradation (e.g., color deviation and low contrast [3]). Therefore, how to restore a clear underwater image is particularly important for the development of the marine industry.

Traditional underwater image enhancement methods can be divided into physical model-free [4]–[8] and physical model-based [9]–[15]. The physical model-free methods mainly adjust the pixel value (e.g., histogram equalization-based

method [8]) to improve the visual quality of the image. However, they ignore the underwater imaging mechanism, resulting in over-enhancement and over-saturation. The physical model-based methods are mainly based on various prior knowledge (e.g., underwater dark channel prior [13]) to estimate underwater imaging parameters (i.e., medium transmission and atmospheric light [16]), and then invert the physical model to obtain enhanced images. They also have limitations: 1) The estimated parameters are based on various prior conditions, but these prior conditions are not always accurate in different underwater environments (e.g., fuzzy prior [17] does not support clear underwater images). 2) It is a great challenge to estimate underwater imaging parameters accurately with physical methods.

In recent years, researchers try to use deep learning-based methods [18]–[23] to enhance underwater images. Perez et al. [18] form a pair of real-world underwater datasets for the first time, and use a simple CNN network to train the mapping relationship between degraded images and reference images. Han et al. [21] propose a deep supervised residual dense network. Wang et al. [22] propose UIEC²-Net, which combines HSV and RGB color spaces, providing new ideas for future work. Although these methods are novel and exciting, their effects are not particularly attractive on the whole. There are two main reasons: 1) Most of them regard contrast enhancement and color restoration as the same, without special treatment of color separately. 2) Most of them neglect the underwater imaging mechanism and rely excessively on the feature learning ability of neural networks.

In order to remedy the above shortcomings, we propose an Adaptive Transmission and Dynamic Color guided network (named ATDCnet) for underwater image enhancement. By observing a large number of underwater datasets, we find that most underwater images are dominated by a single color. To deal with the color deviation problem, we design a Dynamic Color-guided Module (DCM) to post-process the enhanced

This work is supported by Natural Science Foundation of China (Grant No. U20A20196, 62202429) and Zhejiang Provincial Natural Science Foundation of China under Grant No. LR21F020002, LY23F020024.

* The corresponding author.

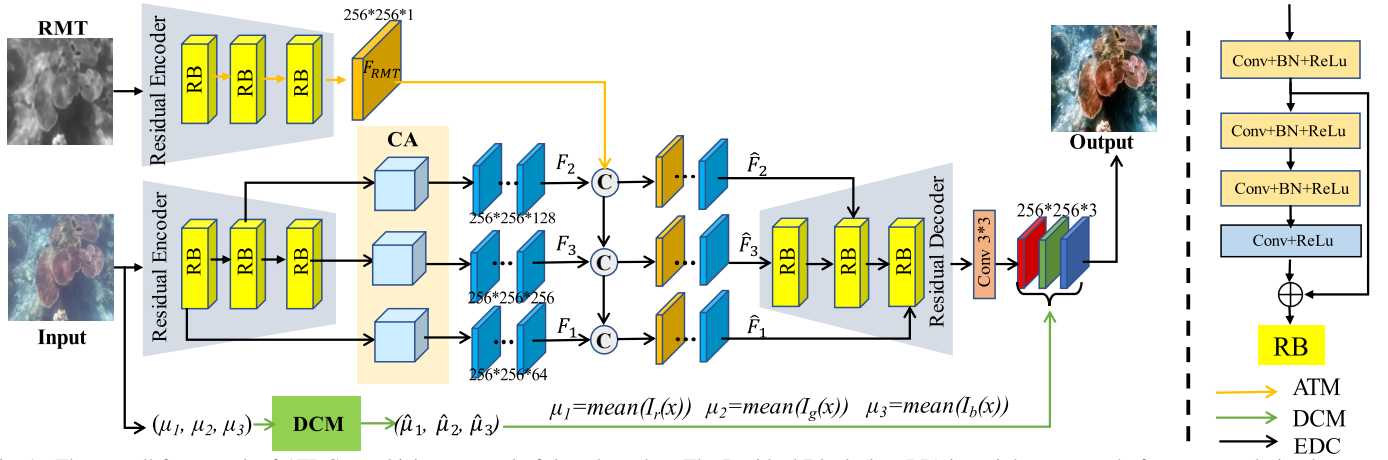


Fig. 1. The overall framework of ATDCnet which composed of three branches. The Residual Block (i.e., RB) is mainly composed of some convolution layer, BatchNorm layer, and LeakyReLU layer. The reverse medium transmission map (denoted as RMT) represents the transmission information of the underwater image. (μ_1, μ_2, μ_3) characterize the general color information of the underwater image.

image color. It can post-process the image color according to different water areas to restore the image color. Secondly, to exploit the knowledge of physics, we design an Adaptive Transmission-directed Module (ATM) to better guide the network. Further, we design an Encoder-Decoder-based Compensation (EDC) structure with attention and a multi-stage feature fusion mechanism to perform color restoration and contrast enhancement simultaneously. The main contributions can be summarized as follows:

- We propose an Adaptive Transmission and Dynamic Color guided network (i.e., ATDCnet) applied for underwater image enhancement. This method focuses on color correction and contrast enhancement of images in different waters.
- To deal with the color deviation problem, we design a Dynamic Color-guided Module (DCM) to post-process the enhanced image color.
- To exploit the knowledge of physics, we design an Adaptive Transmission-directed Module (ATM) guiding the network to better Decoder.
- Extensive experiments on many benchmark datasets demonstrate that our ATDCnet has achieved state-of-the-art in terms of quantitative and visual performance.

II. PROPOSED METHOD

The underwater image degradation process can be represented by the modified Koschmieder light scanning model:

$$I_c(x) = J_c(x)T_c(x) + A_c(1 - T_c(x)), \quad (1)$$

where $I_c(x)$ represents the observed image, $J_c(x)$ denotes the scene radiation, x is the image pixel, A_c defines the global background light, $c = \{r, g, b\}$ means the color channels. $T_c(x) = e^{-\beta_c d(x)}$ represents the transmission value, where β_c is the channel-wise attenuation coefficient depending on water quality, $d(x)$ is the scene depth at pixel x .

In Fig. 1, we show the overall architecture of the proposed network. The network is mainly composed of an

enhancement Encoder-Decoder-based Compensation (EDC) structure, Dynamic Color-guided Module (DCM), and Adaptive Transmission-directed Module (ATM). In the following content, we will briefly introduce the essential parts of our proposed network, mainly including the above three modules and related information fusion mechanisms.

A. Adaptive Transmission-directed Module

Thanks to the powerful feature extraction and representation capabilities of neural networks, we design an Adaptive Transmission-directed module (ATM) to better guide the network. We obtain an initial reverse medium transmission (RMT) map of raw underwater images via a robust general dark channel prior (DCP) [12]. Thus, it is a transmission-guided module which is not necessary to design the loss function of the ATM branch separately. The overall structure is shown in the ATM branch of Fig. 1. It is composed of three cascaded residual blocks, in which the number of channels is 64, 64, and 1 respectively. Using the network optimization method, more accurate transmission information can be obtained.

B. Dynamic Color-guided Module

We design a Dynamic Color-guided module (DCM) to post-process the enhanced image color. By observing a large number of underwater datasets, we find that most underwater images have a single color. In other words, a single color can reflect the general color information of the image. (μ_1, μ_2, μ_3) respectively represent the mean value of the red, green, and blue channels of the underwater image that are obtained by the following formulas:

$$\mu_1 = \text{mean}(I_r(x)), \quad \mu_2 = \text{mean}(I_g(x)), \quad \mu_3 = \text{mean}(I_b(x)), \quad (2)$$

where “mean” denotes the mean operator. Indeed, the global average of underwater image channels represents the overall color information. Therefore (μ_1, μ_2, μ_3) characterize the general color information of the observed underwater image. Then

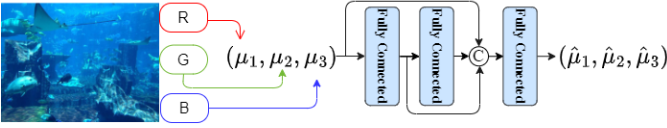


Fig. 2. Details of DCM. The input is the global average of the original underwater image according to the RGB channel, and the corrected attenuation coefficient is obtained after network optimization.

(μ_1, μ_2, μ_3) enter the DCM. After network optimization, three RGB channel color attenuation coefficients $(\hat{\mu}_1, \hat{\mu}_2, \hat{\mu}_3)$ are obtained. Finally, the color is corrected by multiplying the color attenuation coefficient and the feature map. The overall structure of the DCM is shown in Fig. 2, which is composed of three fully connected layers. We concatenate the original input, the output of the first layer, and the output of the second layer according to the channel. This can effectively increase the available information on the network so that a more accurate color attenuation coefficient can be estimated.

C. Encoder-Decoder-based Compensation Structure

In order to preserve the data fidelity and solve the problem of gradient disappearance, we take the residual block, which structure is shown in Fig. 1, as the basic component of the structure. In order to avoid unnecessary information loss, the convolution kernel and stride of all convolution layers are 3×3 and 1 respectively. Such convolution operation will not change the image resolution. In addition, we also introduce the channel-attention (CA) mechanism, by assigning different weights to different channels to highlight more critical features. In the decoder stage, in order to make full use of the features of different stages (F_1, F_2, F_3 in Fig. 1), we design a multi-stage feature fusion mechanism. With the help of the attention mechanism, multi-stage features can increase more available information for the network, thus improving the network's performance.

D. Loss Function

In order to achieve an effective balance between visual quality and quantitative scores, we adopt a linear combination of ℓ_2 loss, perceptual loss, and SSIM loss. Specifically, ℓ_2 loss measures the ℓ_2 distance between the reconstructed image J and the reference image \hat{J} :

$$L_{\ell_2} = \frac{1}{N} \sum_{i=1}^N \|\hat{J}_i - J_i\|_2, \quad (3)$$

where J_i represents the pixel value at the reconstructed image position i , \hat{J}_i represents the pixel value at the reference image position i . Since ℓ_2 loss is difficult to capture high-level semantics, we introduce perceptual loss to evaluate the visual quality of images. It measures the ℓ_1 distance between the reconstructed image J and the reference image \hat{J} in the feature space defined by VGG-19:

$$L_{perc} = \frac{1}{C_k H_k W_k} \sum_{i=1}^N \|\phi_k(J_i) - \phi_k(\hat{J}_i)\|_1, \quad (4)$$

TABLE I
ABLATION STUDY OF DIFFERENT SETTINGS, I.E., W/O CA AND W/O $\hat{F} := (F_1, F_3)$.

Type	Model	PSNR \uparrow	SSIM \uparrow	UCIQE \uparrow
A	w/o CA, w/o \hat{F}	19.92	0.89	0.67
B	w/o CA, with \hat{F}	19.59	0.89	0.67
C	with CA, w/o \hat{F}	22.93	0.92	0.72
D	Ours	23.43	0.92	0.74

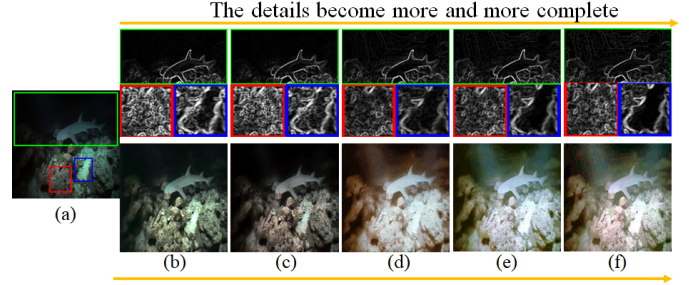


Fig. 3. Ablation study of CA and \hat{F} of EDC on UIEB dataset. (a) Input. (b) w/o CA + w/o \hat{F} . (c) w/o CA + with \hat{F} . (d) with CA + w/o \hat{F} . (e) ours. (f) Ground Truth. The first row is the gradient map of the enhanced image, and the second row is the enhanced image. The EDC with CA and \hat{F} produces clearer and more complete image details.

where ϕ_k represents the k_{th} convolutional layer. N is the number of each batch in the training phase. C_k, H_k, W_k represents the channel number, height, and width of the feature map at layer k of the VGG-19 network respectively. In our experiment, we calculate the perceptual loss at layer $relu5_3$ of the VGG-19 network. In order to maintain the similarity of structure and texture between the reconstructed image J and the reference image \hat{J} , we introduce SSIM loss:

$$L_{SSIM} = 1 - \frac{1}{N} \sum_{i=1}^N SSIM(J_i, \hat{J}_i), \quad (5)$$

all losses act on the output stage of the network, and the total loss finally used for the training phase is expressed as follows:

$$L_{total} = \alpha L_{\ell_2} + \beta L_{perc} + \gamma L_{SSIM}, \quad (6)$$

according to experience, we set α, β , and γ as 1, 0.01, and 100 respectively.

III. EXPERIMENTS

A. Setups

Datasets. We evaluate the performance of the proposed method on two types of datasets: the first type has reference images (e.g., EUVP [24], UIEB [19], LSUI [25], UFO-120 [26]); The other is without reference image (e.g., C60 [19], RUIE [27], SQUID [28]).

Metrics. We use three commonly used image evaluation metrics (i.e., Mean Square Error (MSE), Peak Signal to Noise Ratio (PSNR), and Structure Similarity Index (SSIM)) to compare different methods quantitatively. A higher PSNR or SSIM means that the enhanced image is closer to nature in

TABLE II
ABLATION STUDY OF THE FRAMEWORK COMPONENTS ON UIEB DATASET

Settings	EDC	ATM	DCM	PSNR↑	SSIM↑	UIQM↑
(i)	✓			22.79	0.91	4.08
(ii)	✓	✓		23.29	0.92	4.10
(iii)	✓		✓	22.91	0.91	4.15
(iv)	✓	✓	✓	23.43	0.92	4.29

terms of vision and structure. A lower MSE means that the image has a better reconstruction effect. In addition, we also introduce non-reference Underwater Image Quality Measure (UIQM) [29] and Underwater Color Image Quality Evolution (UCIQE) [30]. A higher UIQM or UCIQE represents a better human visual perception.

B. Ablation Study

In this section, we will conduct ablation experiments in two kinds to study the role of each module. In the first kind, only the enhancement EDC structure is ablated ATM and DCM are fixed; In the second kind, ATM and DCM are ablated (EDC is fixed).

Channel-attention (CA) + feature ($\hat{F} := (\hat{F}_1, \hat{F}_3)$). EDC is responsible for contrast enhancement and color restoration in our method. In order to improve the performance of this module, we introduce the CA and $\hat{F} := (\hat{F}_1, \hat{F}_3)$. We conduct ablation experiments on EDC separately, and the experimental results are shown in Table I. Table I A and B show that without CA, \hat{F} will damage the model’s performance. Table I A and C show that the network performance has been greatly improved, which indicates that CA effectively helps the network select more critical features. Table I C and D illustrate that \hat{F} will retain key features after CA screening. As can be seen, Fig. 3(e) with CA and \hat{F} has more complete image details.

EDC + ATM. We combine the transmission information to better guide the EDC to enhance the image. Observing Table II (i) and (ii), PSNR and SSIM have improved significantly. However, the improvement of the visual effect is not obvious after observing Fig. 4 (EDC) and Fig. 4 (EDC+ATM). In low-level visual tasks, a high PSNR or SSIM does not necessarily represent a good image visual effect. After the introduction of the ATM, although the reconstruction effect has been improved (e.g. PSNR and SSIM have been improved), these reconstructed pixels do not necessarily conform to human visual perception.

EDC + DCM. We conduct post-processing on the enhanced image color. In Table II, by comparing Table II (ii) and (iii), we can see that UIQM has been effectively improved. Comparing Fig. 4 (EDC+ATM) and Fig. 4 (EDC+DCM), it can be seen that DCM has the ability to restore image color.

EDC + ATM + DCM. According to Table II (iv), after combining the three modules, various metrics have been significantly improved. We believe that this is the result of the assistance between the three modules. After the introduction of the ATM, the image reconstruction effect is improved, but these reconstructed pixels do not conform to human visual

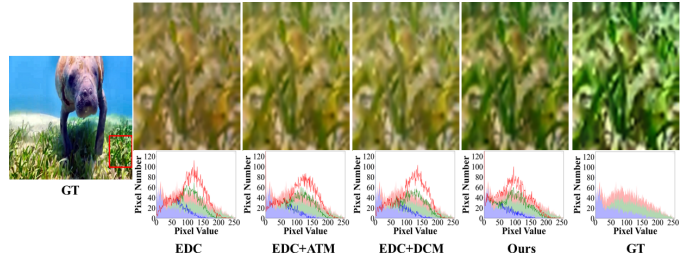


Fig. 4. Ablation study of the ATM and DCM on UIEB dataset. It can be seen from the pixel distribution map (The abscissa is the pixel value, and the ordinate is the number of pixels) that the complete model (Ours) with ATM and DCM is closer to Ground Truth.

perception. When the DCM is added, it can assist the ATM to reconstruct pixels better. The reconstructed pixel has both a better visual and reconstruction effect, so the final image will be more natural. Looking at Fig. 4 (Ours) and Fig. 4 (GT), the enhanced image is very close to the reference image.

C. Comparison Results

We make quantitative and qualitative comparisons with eight state-of-the-art methods, including traditional methods (e.g., UDCP [13], Fusion [7]), CNN-based methods (e.g., Water-Net [19], Ucolor [31], USUIR [32], PUIE-Net [33]), and GAN-based methods (e.g., UGAN [34], FUnIE-GAN [24]) on seven datasets.

Quantitative comparison. We test the supervised metrics in four underwater datasets (i.e., EUVP, UIEB, LSUI, UFO-120). The average scores of MSE, PSNR, and SSIM are presented in Table III. As shown in Table III, in each line, we use black bold to indicate the best and underline to indicate the second. First of all, it is obvious that the average score of our design method is much higher than other methods. Secondly, the robustness of these state-of-the-art methods is uneven (e.g., FUnIE-GAN performs poorly on LSUI but better on the other three datasets). On the contrary, our method can be well generalized on all datasets.

In addition, we also conduct experiments on challenging datasets (i.e., C60, RUIE, SQUID). The results are presented in Table IV. Looking at Table IV, our method obtains two first (UIQM: C60 and RUIE) and two seconds (UCIQE: C60. UIQM: SQUID). In general, our method has better generalization performance than other methods. In addition, We find that although the traditional methods (e.g., Fusion) have lower supervised metrics (e.g., PSNR), they have higher unsupervised metrics (e.g., UCIQE).

Qualitative Comparisons. In Fig. 5, we provide the enhanced results of the designed method and the method with relatively high PSNR and SSIM scores (i.e., Fusion [7], FUnIE-GAN [24], Ucolor [31], PUIE-Net [33], USUIR [32]) in Table III. It can be seen from Fig. 5 that the traditional method (e.g., Fusion [7]) has over-enhanced the image; The image contrast enhanced by the GAN-based method (e.g., FUnIE-GAN [24]) is obviously insufficient. The CNN-based methods (e.g., USUIR [32], PUIE-Net [33]) have significantly

TABLE III
QUANTITATIVE RESULTS IN FOUR DIFFERENT UNDERWATER DATASETS (I.E., EUVP, UIEB, UFO-120, LSUI).

Datasets	Metrics	UDCP	Fusion	Water-Net	UGAN	FUnIE-GAN	Ucolor	USUIR	PUIE-Net	Ours
EUVP	PSNR \uparrow	16.38	17.61	20.14	23.51	<u>23.54</u>	21.89	23.52	22.60	25.62
	SSIM \uparrow	0.64	0.75	0.68	<u>0.81</u>	<u>0.81</u>	0.79	<u>0.81</u>	<u>0.81</u>	0.87
	MSE \downarrow	1990	1331	826	401	<u>398</u>	505	<u>399</u>	438	239
UIEB	PSNR \uparrow	13.05	17.60	19.11	20.17	<u>20.68</u>	20.63	20.31	20.36	23.43
	SSIM \uparrow	0.62	0.77	0.79	0.82	<u>0.72</u>	0.84	0.84	<u>0.88</u>	0.92
	MSE \downarrow	3779	1331	1220	874	752	770	804	<u>730</u>	416
UFO-120	PSNR \uparrow	18.26	14.58	22.46	23.45	<u>25.15</u>	21.04	17.45	21.62	25.23
	SSIM \uparrow	0.72	0.54	0.79	<u>0.80</u>	0.82	0.66	0.69	0.74	0.82
	MSE \downarrow	1249	2968	458	393	<u>253</u>	599	1327	514	232
LSUI	PSNR \uparrow	12.66	14.48	17.73	19.79	<u>19.37</u>	21.56	18.64	<u>22.48</u>	26.02
	SSIM \uparrow	0.62	0.79	0.82	0.78	<u>0.84</u>	<u>0.84</u>	0.82	0.91	0.91
	MSE \downarrow	4529	3501	1361	883	946	563	1025	<u>493</u>	238

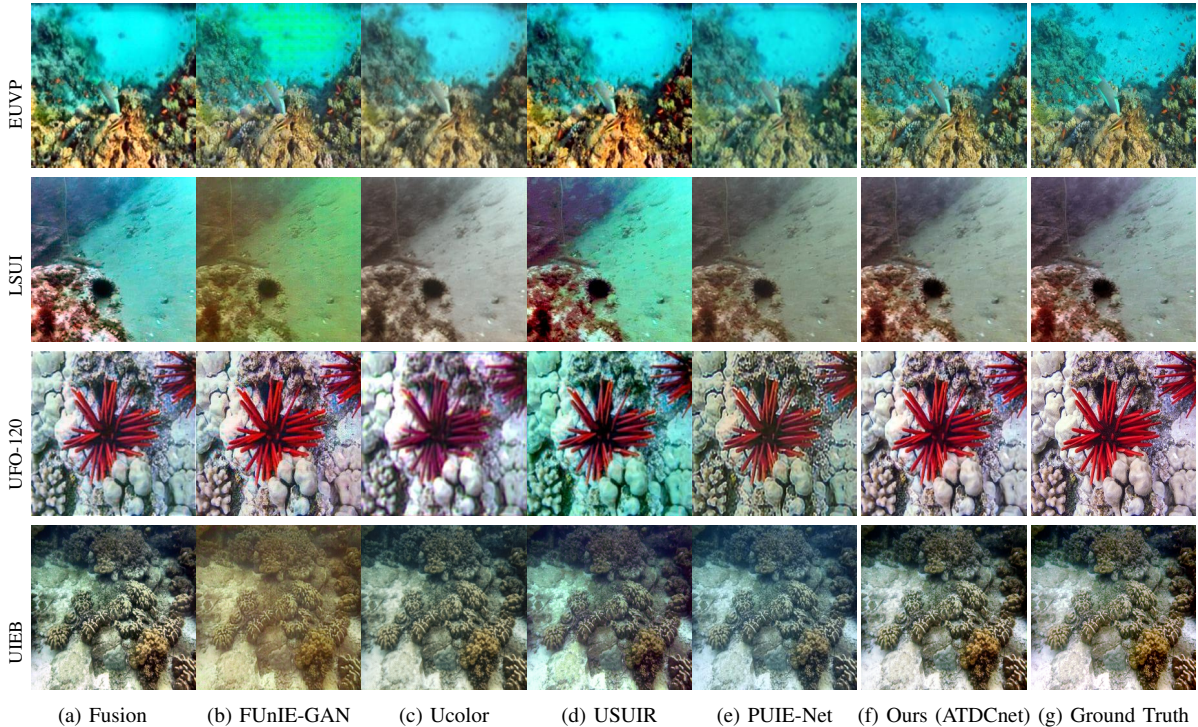


Fig. 5. Visual comparison with different underwater image enhancement methods on real-world datasets (i.e., EUVP, LSUI, UFO-120, UIEB).

improved the contrast, but the image color has not been effectively restored. On the contrary, our enhanced image is more attractive in terms of color and contrast. Due to space limitations, we provide more qualitative analysis in the supplementary materials.

IV. CONCLUSION

We propose a new underwater image enhancement model. On the basis of improving image contrast by the Encoder-Decoder-based Compensation (EDC) structure, the deep processing of color is realized by the Dynamic Color-guided Module (DCM). In addition, domain knowledge is incorporated into the network through the Adaptive Transmission-directed Module (ATM). Extensive experiments on different benchmark datasets have proved the superiority of our solution. The

ablation study verified the effectiveness of the key components of our method.

REFERENCES

- [1] Geoffrey N Bailey and Nicholas C Flemming, "Archaeology of the continental shelf: marine resources, submerged landscapes and underwater archaeology," *Quaternary Science Reviews*, vol. 27, no. 23-24, pp. 2153–2165, 2008.
- [2] M Dubreuil, P Delrot, Isabelle Leonard, Ayman Alfalou, Christian Brosseau, and Aristide Dogariu, "Exploring underwater target detection by imaging polarimetry and correlation techniques," *Applied Optics*, vol. 52, no. 5, pp. 997–1005, 2013.
- [3] Kai Hu, Chenghang Weng, Yanwen Zhang, Junlan Jin, and Qingfeng Xia, "An overview of underwater vision enhancement: From traditional methods to recent deep learning," *Journal of Marine Science and Engineering*, vol. 10, no. 2, pp. 241, 2022.
- [4] Weidong Zhang, Lili Dong, and Wenhai Xu, "Retinex-inspired color correction and detail preserved fusion for underwater image enhancement," *Computers and Electronics in Agriculture*, vol. 192, pp. 106585, 2022.

TABLE IV
AVERAGED UNSUPERVISED SCORES (I.E., UIQM, UCIQE) ON
REAL-WORLD UNDERWATER DATASETS (I.E., C60, RUIE, SQUID)
WITHOUT REFERENCE IMAGES.

Methods	C60		RUIE		SQUID	
	UIQM ↑	UCIQE ↑	UIQM ↑	UCIQE ↑	UIQM ↑	UCIQE ↑
UDCP	5.55	0.65	5.34	0.60	4.96	0.59
Fusion	5.79	0.76	5.41	0.76	5.35	0.79
Water-Net	5.63	0.66	4.69	0.62	5.25	0.47
UGAN	5.67	0.67	5.13	0.64	5.30	0.44
FUnIE-GAN	5.79	0.68	5.13	0.66	5.35	0.46
Ucolor	<u>5.80</u>	0.67	5.40	0.63	5.79	0.51
USUIR	5.70	0.68	<u>5.48</u>	<u>0.75</u>	5.18	<u>0.66</u>
PUIE-Net	5.46	0.62	4.94	0.59	5.56	0.52
Ours	5.83	<u>0.70</u>	5.57	0.69	<u>5.69</u>	0.55

- [5] Codruta O Ancuti, Cosmin Ancuti, Christophe De Vleeschouwer, and Philippe Bekaert, "Color balance and fusion for underwater image enhancement," *IEEE Transactions on Image Processing*, vol. 27, no. 1, pp. 379–393, 2017.
- [6] Xueyang Fu, Peixian Zhuang, Yue Huang, Yinghao Liao, Xiao-Ping Zhang, and Xinghao Ding, "A retinex-based enhancing approach for single underwater image," in *2014 IEEE International Conference on Image Processing (ICIP)*. IEEE, 2014, pp. 4572–4576.
- [7] Cosmin Ancuti, Codruta Ormiana Ancuti, Tom Haber, and Philippe Bekaert, "Enhancing underwater images and videos by fusion," in *2012 IEEE Conference on Computer Vision and Pattern Recognition (CVPR)*. IEEE, 2012, pp. 81–88.
- [8] Muhammad Suzuri Hitam, Ezmahamrul Afreen Awalludin, Wan Nural Jawahir Hj Wan Yusoff, and Zainuddin Bachok, "Mixture contrast limited adaptive histogram equalization for underwater image enhancement," in *2013 International Conference on Computer Applications Technology (ICCAT)*. IEEE, 2013, pp. 1–5.
- [9] Chong-Yi Li, Ji-Chang Guo, Run-Min Cong, Yan-Wei Pang, and Bo Wang, "Underwater image enhancement by dehazing with minimum information loss and histogram distribution prior," *IEEE Transactions on Image Processing*, vol. 25, no. 12, pp. 5664–5677, 2016.
- [10] Adrian Galdran, David Pardo, Artzai Picón, and Aitor Alvarez-Gila, "Automatic red-channel underwater image restoration," *Journal of Visual Communication and Image Representation*, vol. 26, pp. 132–145, 2015.
- [11] Yi Wang, Hui Liu, and Lap-Pui Chau, "Single underwater image restoration using adaptive attenuation-curve prior," *IEEE Transactions on Circuits and Systems I: Regular Papers*, vol. 65, no. 3, pp. 992–1002, 2017.
- [12] Yan-Tsung Peng, Keming Cao, and Pamela C Cosman, "Generalization of the dark channel prior for single image restoration," *IEEE Transactions on Image Processing*, vol. 27, no. 6, pp. 2856–2868, 2018.
- [13] Paulo LJ Drews, Erickson R Nascimento, Silvia SC Botelho, and Mario Fernando Montenegro Campos, "Underwater depth estimation and image restoration based on single images," *IEEE Computer Graphics and Applications*, vol. 36, no. 2, pp. 24–35, 2016.
- [14] Haotian Qian, Wentao Tong, Pan Mu, Zheyuan Liu, and Hanning Xu, "Real-world underwater image enhancement via degradation-aware dynamic network," in *PRICAI 2022: Trends in Artificial Intelligence: 19th Pacific Rim International Conference on Artificial Intelligence, PRICAI 2022, Shanghai, China, November 10–13, 2022, Proceedings, Part III*. Springer, 2022, pp. 530–541.
- [15] Risheng Liu, Pan Mu, Jian Chen, Xin Fan, and Zhongxuan Luo, "Investigating task-driven latent feasibility for nonconvex image modeling," *IEEE Transactions on Image Processing*, vol. 29, pp. 7629–7640, 2020.
- [16] Saeed Anwar and Chongyi Li, "Diving deeper into underwater image enhancement: A survey," *Signal Processing: Image Communication*, vol. 89, pp. 115978, 2020.
- [17] Yan-Tsung Peng and Pamela C Cosman, "Underwater image restoration based on image blurriness and light absorption," *IEEE Transactions on Image Processing*, vol. 26, no. 4, pp. 1579–1594, 2017.
- [18] Javier Perez, Aleks C Attanasio, Nataliya Nechyporenko, and Pedro J Sanz, "A deep learning approach for underwater image enhancement," in *International work-conference on the interplay between natural and artificial computation*. Springer, 2017, pp. 183–192.
- [19] Chongyi Li, Chunle Guo, Wenqi Ren, Runmin Cong, Junhui Hou, Sam Kwong, and Dacheng Tao, "An underwater image enhancement benchmark dataset and beyond," *IEEE Transactions on Image Processing*, vol. 29, pp. 4376–4389, 2019.
- [20] Chongyi Li, Saeed Anwar, and Fatih Porikli, "Underwater scene prior inspired deep underwater image and video enhancement," *Pattern Recognition*, vol. 98, pp. 107038, 2020.
- [21] Yanling Han, Lihua Huang, Zhonghua Hong, Shouqi Cao, Yun Zhang, and Jing Wang, "Deep supervised residual dense network for underwater image enhancement," *Sensors*, vol. 21, no. 9, pp. 3289, 2021.
- [22] Yudong Wang, Jichang Guo, Huan Gao, and Huihui Yue, "Uiec²-net: Cnn-based underwater image enhancement using two color space," *Signal Processing: Image Communication*, vol. 96, pp. 116250, 2021.
- [23] Pan Mu, Haotian Qian, and Cong Bai, "Structure-inferred bi-level model for underwater image enhancement," *Proceedings of the 30th ACM International Conference on Multimedia (MM)*, 2022.
- [24] Md Jahidul Islam, Youya Xia, and Junaed Sattar, "Fast underwater image enhancement for improved visual perception," *IEEE Robotics and Automation Letters*, vol. 5, no. 2, pp. 3227–3234, 2020.
- [25] Lintao Peng, Chunli Zhu, and Liheng Bian, "U-shape transformer for underwater image enhancement," *arXiv preprint arXiv:2111.11843*, 2021.
- [26] Md Jahidul Islam, Peigen Luo, and Junaed Sattar, "Simultaneous enhancement and super-resolution of underwater imagery for improved visual perception," *arXiv preprint arXiv:2002.01155*, 2020.
- [27] Risheng Liu, Xin Fan, Ming Zhu, Minjun Hou, and Zhongxuan Luo, "Real-world underwater enhancement: Challenges, benchmarks, and solutions under natural light," *IEEE Transactions on Circuits and Systems for Video Technology*, vol. 30, no. 12, pp. 4861–4875, 2020.
- [28] Dana Berman, Deborah Levy, Shai Avidan, and Tali Treibitz, "Underwater single image color restoration using haze-lines and a new quantitative dataset," *IEEE Transactions on Pattern Analysis and Machine Intelligence*, vol. 43, no. 8, pp. 2822–2837, 2020.
- [29] Karen Panetta, Chen Gao, and Sos Agaian, "Human-visual-system-inspired underwater image quality measures," *IEEE Journal of Oceanic Engineering*, vol. 41, no. 3, pp. 541–551, 2015.
- [30] Miao Yang and Arcot Sowmya, "An underwater color image quality evaluation metric," *IEEE Transactions on Image Processing*, vol. 24, no. 12, pp. 6062–6071, 2015.
- [31] Chongyi Li, Saeed Anwar, Junhui Hou, Runmin Cong, Chunle Guo, and Wenqi Ren, "Underwater image enhancement via medium transmission-guided multi-color space embedding," *IEEE Transactions on Image Processing*, vol. 30, pp. 4985–5000, 2021.
- [32] Zhenqi Fu, Huangxing Lin, Yan Yang, Shu Chai, Liyan Sun, Yue Huang, and Xinghao Ding, "Unsupervised underwater image restoration: From a homology perspective," in *Proceedings of the AAAI Conference on Artificial Intelligence (AAAI)*, 2022, vol. 36, pp. 643–651.
- [33] Zhenqi Fu, Wu Wang, Yue Huang, Xinghao Ding, and Kai-Kuang Ma, "Uncertainty inspired underwater image enhancement," in *European Conference on Computer Vision (ECCV)*. Springer, 2022, pp. 465–482.
- [34] Cameron Fabbri, Md Jahidul Islam, and Junaed Sattar, "Enhancing underwater imagery using generative adversarial networks," in *2018 IEEE International Conference on Robotics and Automation (ICRA)*. IEEE, 2018, pp. 7159–7165.